This article has been accepted for publication in a future issue of this journal, but has not been fully edited. Content may change prior to final publication. Citation information: DOI 10.1109/TIM.2020.3005258, IEEE Transactions on Instrumentation and Measurement

Anchor Calibration for Real-Time-Measurement Localization Systems

Peter Krapež and Marko Munih

***Abstract*—This paper investigates the effect of additional calibration modules in a 3D real-time localization system during the calibration of anchor position. A quick calibration is desirable for new anchors that are positionally undetermined in the working coordinate system.**

Three localization methods were tested for the anchor calibration: multi-dimensional scaling, semi-definite programming, and iterative tri-lateration. First, the accuracy of the anchor localization was studied by simulating a change in the number of additional calibration modules and their positions. Second, tests on a real system with ultra-wideband modules were performed to validate the improvements in the anchor calibration when using the additional calibration modules.

The experimental results revealed an improvement in the anchor localization for all three methods, where the average positional error was improved by 0.01 m in the first, and by 0.30 m in the second, scenario. The MDS method had the best absolute performance, with an average positional error that was as much as two times less in comparison with the other two methods. This investigation demonstrates that the positional error can be successfully reduced by using additional calibration modules. The calibration of anchor positions in the working coordinate system using additional calibration modules resulted in a 3D error of less than 0.32 m.

***Index Terms*—Anchor calibration, 3D anchor localization, calibration modules, position measurement, ToF, ultra-wideband technology.**

I. Introduction

Autonomous mobile applications used in everyday life and the localization demands of the Internet of Things are increasing. These include automatic lawn mowers, drones [1], AGVs, smart sensors [2] and even automated forklifts that leave the production site's doors to load a truck. Real-time localization based on radio tri-lateration requires a number of radio anchors. To extend the range, new anchors are needed, together with calibration of the anchor position in space. Even changes in the working site may require anchor re-positioning and, consequently, a new anchor calibration. This is the advantage of localization systems with automatic anchor calibration.

In real-time localization systems (RTLSs) the mobile unit is localized by measuring the distances to static modules, i.e., anchors, with a known position. The positions of the anchors can be determined in two ways. The first option is to measure the anchor position with a measuring system such as a tachymeter, utilizing geodetic procedures. An alternative is to calibrate the anchor position by measuring inter-module distances and computing the locations with mathematical algorithms. Although the use of external measurement equipment provides anchor positions with high accuracy, the anchors have to be constructed and placed in such a way that enables an external measurement, which means the ability to reconfigure is reduced. The second anchor-calibration approach represents an effortless method for anchor localization and could contribute to RTLSs as a turnkey product where the end-user can do the entire setup of the RTLS without additional equipment.

Numerous indoor RTLSs are presented in literature and are available as products [3]. Authors in [4] presented RTLS based on ultra-wideband (UWB) technology for asynchronous time difference of arrival localization. Kolakowski et al. [5] developed a hybrid system where UWB is used for the first-time calibration of Bluetooth Low Energy RTLS. Wang et al. [6] used UWB as a secondary system for frequent calibration of primary RTLS based on K-band Doppler radar sided with a gyroscope. Authors in [7], [8] presented localization in a harsh industrial environment. All of RTLSs mentioned above uses anchors system, with known positions, for localizing mobile modules.

A lot of work was carried out in another domain, i.e., mobile sensor localization without the use of anchor modules. The problem is the same as a stationary anchor calibration, because in both cases no anchor modules with known positions are present. The localization of new modules can be conducted with a global approach. In this case the positions of the old and new modules are calculated simultaneously and updated for the old and new modules. An alternative to that is the iterative approach, where only the positions of the new modules are defined.

Previous work relied on multi-dimensional scaling (MDS) [9], [10] as one of the global approaches to module localization. Shang *et al.* [11] presented a method that uses only the connectivity information between the modules. The authors implemented different approaches to constructing and refining the Euclidian distance matrix (EDM), where all the approaches share a common course of first acquiring the EDM and then using the MDS to compute the relative module coordinates. Optionally, if more then three module positions are known, the relative module coordinates can be transformed to the global coordinate system. Another global approach is to use semi-definite programming (SDP), shown in [12], [13], while in [13] the EDM completion problem is addressed.

An iterative localization algorithm called sweep is explained in [14], where the iterative tri-lateration is replaced by bi-

Peter Krapež, Marko Munih are with Laboratory of robotics, University of Ljubljana, Faculty of Electrical Engineering, Tržaška cesta 25, Ljubljana, Slovenia, e-mail: peter.krapez@fe.uni-lj.si, e-mail: marko.munih@robo.fe.uni-lj.si

Peter Krapež is the corresponding author.

lateration, so more modules can be localized. In this way, two possible locations for each new module are computed. All the possible locations are then included in the localization of the next modules, which results in a rapidly expanding number of solutions. The authors show how to reduce the number of possible module solutions by eliminating the least-suitable ones. Priyantha *et al.* [15] presented a distributed localization algorithm for a network of sensors with the use of mass-spring optimization. Another distributed algorithm is shown in [16], where newly computed module coordinates are added to a set of already-localized modules.

Localization algorithms were used in the past for anchor calibrations in RTLSs. Kuang *et al.* [17] solved the localization problem by factorizing a compaction matrix, which contains information about the distances between anchor modules. The minimal non-iterative solvers for the second and third space dimensions were explored. Here, the number of transmitting and receiving anchors are defined for each solver. Batstone *et al.* [18] used factorization of a compaction matrix, adopting the rank constraints of the compaction matrix for outlier detection. They are focused on problems with missing distances and outliers in real-time anchor calibration. The authors approached this problem by solving smaller graph problems and aligning their coordinate systems to create a global solution. The transformation was computed from the overlapping areas of smaller graphs.

Zhou *et al.* [19] presented an anchor calibration for the rotational time-difference-of-arrival and the MDS algorithm. The authors showed that the MDS's accuracy rapidly increases when the number of anchors increases to ten. The algorithm for the anchor calibration presented in [20] computes more solutions with a solver using multi-dimensional, nonlinear least-squares fitting. Based on three fitness functions, the final solution is selected from different initial positions.

The application of an anchor calibration using a sweep algorithm was made by Nakamura *et al.* [21]. By applying fully-connected quadrilaterals from [22], the anchors were uniquely localized. The authors used tri-lateration for the anchor calibration from three selected anchors, which define the coordinate system. Using a method called robust quad check, no flip and flex ambiguities were ensured, which in turn improved the tri-lateration algorithm.

The authors in [23] and [24] introduced a new feature in the process of anchor calibration. An additional anchor (a new calibration module or temporary anchor) is used just for the purposes of anchor calibration. Müller *et al.* [23] presented an anchor-calibration method that uses bi-lateration. First, the seed anchors were computed, then all of the other anchors were sorted in bi-lateration ordering and their positions were computed with bi-lateration. For each configuration, the stress is computed and the best configuration is selected for the end result. The authors implemented a temporary anchor, which was placed in the system in a way that ranging using all of the anchors was possible. After the anchor calibration is completed, a temporary anchor is removed from the anchor system. With the temporary anchor placement, new measurements are added to the collection of inter-module distances so that the anchors without line-of-sight (LOS) can be localized.

Van de Velde *et al.* [24] introduced a technique similar to the simultaneous localization and mapping (SLAM) method. Rather than using sensors to scan the surroundings, it uses radio communications for the ranging between anchors. They used a calibration unit (CU) that was moved in space by the operator in order to collect the distance measurements between the anchors and the CU. When the CU is moved in a straight line, all the inter-module distances between the anchors can be computed, and by means of weighted least squares, the anchors' coordinates can be determined.

As outlined above, previous studies looked at different methods of anchor calibration, with most of the research focused on 2D localization problems. This paper investigates the problem of anchor localization in 3D space by placing localized anchors in a working coordinate system. The possibility to decrease the anchors' localization error was explored through the use of an additional calibration unit that contains calibration modules (CMs) with known relative positions with respect to each other. In this research, the methods MDS, SDP [13] and an algorithm based on tri-lateration (TRI) [14], [20], [23] were compared. A series of simulations was executed first to evaluate the impact that the calibration unit has on the anchor-localization error. Then, experiments on a real system for two scenarios with LOS and non-line-of-sight (NLOS) conditions were performed to validate the simulation results. The anchor calibration implemented four calibration modules on the CU to provide several possibilities for the proposed calibration method. The final goal of this work was to evaluate and present an anchor-calibration method for improved anchor localization in an arbitrary coordinate system. To the best of our knowledge, this is the first attempt to examine the effect of implementing a new CU in an anchor calibration in terms of an anchor-localization error. The anchor was localized in a specific coordinate system, and, most importantly, in 3D, not only a planar system.

II. Anchor-calibration method with a calibration unit

To operate a RTLS the positions of the anchors in a common working coordinate system must be known. Anchor calibration is a process of determining the anchors' relative positions from the measured distances between all the anchors and transforming them into a global (working) coordinate system. From N anchor modules, $M = \binom{N}{2}$ inter-module distances are measured, which are part of an EDM with a size of $N \times N$. The anchors' positions are obtained by minimizing the error:

$$e_{ij} = \left\| a_i - a_j \right\| - d_{ij}, \tag{1}$$

where a_i and a_j are the positions of the anchors and d_{ij} is the measured distance between the i-th and the j-th anchor.

The final positional error of the mobile unit in the RTLS is a superposition of not only the distance measurement error between the anchors and the mobile unit, but also the positional error arising from the placement of the anchors used in the RTLS. Therefore, decreasing the anchor's positional error and improving the anchor's position in a working coordinate system based on an anchor calibration is the motivation for this work.

When designing the RTLS, the best conditions, within the environment constraints in which it will operate, are desired for radio communications between the anchors and the mobile unit modules. Such conditions are usually ensured by placing the anchors at elevated positions (Fig. 1), so that the radio signal is not obstructed by people moving around and other obstacles. With the aforementioned anchor configuration, the modules are not deployed through the full possible height range of the RTLS setup. Therefore, a setup that includes the CU and places it on the floor has been adopted. In this way the entire range of distances in the z-axis is covered (green dots in Fig. 1) and the full spatial information about the space in which the RTLS operates is ensured. The idea of the CU

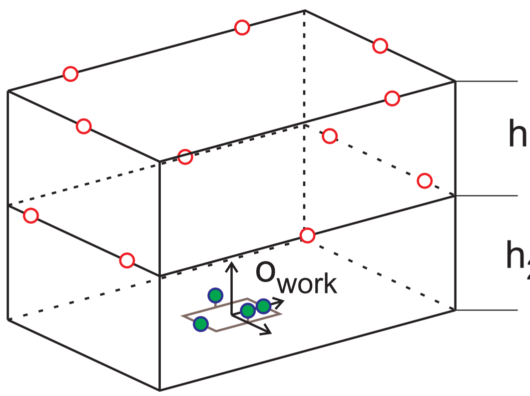

Fig. 1. Anchor calibration with calibration unit.

is introduced in [23] and [24], but the purpose of the CU in this paper is different. Here, the CU is implemented and tested as a calibration method for initializing the new RTLS setup and localizing the new anchors in a defined working coordinate system (Fig. 1), where no prior information about the anchors' positions is available. With the CU placed correctly, the minimum positional error of the anchors is achieved. The CU in our case is placed in such a way that the relation to the working coordinate system is known. The computed positions of the anchors are then aligned with the CU, so placing them in the working coordinate system.

In this paper the anchor-calibration method in 3D is validated. It can be used for localizing the anchors in an arbitrary working coordinate system with additional calibration modules. The method can be adopted for scenarios where not all the anchors are in each others' radio ranges. Smaller anchor configurations are localized independently of each other and afterwards, an alignment with the common anchors is performed.

III. System description

A. UWB modules

The test system consists of 18 printed-circuit boards with UWB DWM1000 modules, a STM32L4 microprocessor and a USB port (Fig. 2). The modules are enclosed in a protective plastic housing and can be placed in any position with a customized attachment plate.

After all the anchors are placed in the desired configuration, the master anchor is connected to the PC via the USB (Fig. 3).

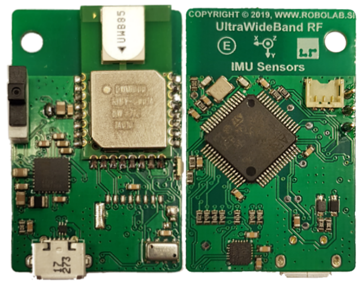

Fig. 2. Top and bottom sides of the designed board with the UWB radio module.

All the incoming and outgoing data from the PC to the anchors and vice-versa is relayed through the master anchor.

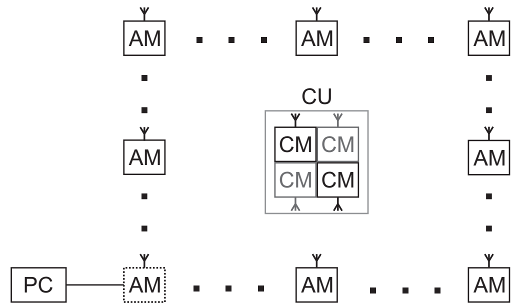

Fig. 3. System configuration block diagram.

B. Distance measurements

The distances between the modules were computed using the time-of-flight (ToF) method for the radio signal traveling between two modules. For the ToF calculation a two-way-ranging equation was used [25]. After the modules' deployment, all the inter-module distances were measured, as described in Algorithm 1. For the experiment the decision was

Algorithm 1 distance measurements of one set

```
Initialization list = all anchor and CU addresses
for all addresses in list do
    for all addresses in list do
        gather 250 distance measurements
        send measurements to master anchor
        send measurements to PC
    end for
end for
Finalization build EDM from distance measurements
```

made to have 40 measurement sets for system and calibration method stability analysis. The measurements were then filtered for any outliers and passed to the localization algorithms for processing. The outlier filtering involved applying a threshold for the Mahalanobis distance for each sample. The filtered values were replaced with a mean value before the filtration, so the number of samples remained the same after the filtering [26].

This article has been accepted for publication in a future issue of this journal, but has not been fully edited. Content may change prior to final publication. Citation information: DOI 10.1109/TIM.2020.3005258, IEEE Transactions on Instrumentation and Measurement

C. UWB module calibration

A calibration was made for each pair of anchor and CM in the same experimental environment. The calibration measurements were taken from 1 to 32 m in 1-m increments. Several regressions were made on the measured data. Since all the modules had similar error characteristics, a higher order of polynomial regression was used. The best fit was with the 6^{th} order of polynomial regression. An average RMSE of 0.03 m was obtained for all 180 calibration regressions. The average distance error over all the distance measurements and all the measurement sets after the calibration was 0.07 m. The authors of [1] suggested the calibration of the UWB modules with linear regression for two intervals with the ranges 0–1.5 m and 1.5–8 m. Due to the decreasing accuracy of the measurements to 1.5 m, we used the same 6^{th}-order polynomial regression for the entire calibration distance.

IV. Methodology

A. Performance metrics

Two performance metrics are presented. The first metric is determining the quality of fit between the localization and the measured datasets. The second metric is used to evaluate the error between the calculated and the reference coordinates.

The mean square error distance or stress can be defined as:

$$Stress = \sqrt{\frac{\sum_{i=1}^{M} (\hat{d}_i - d_i)^2}{d_i}} \tag{2}$$

where M is the number of inter-module distances for N modules, $\hat{d}_i$ is the distance calculated from the localization algorithms, and d_i is the measured distance or the distance from the simulation. Stress is used in the algorithm as an internal performance metric in the TRI localization method.

The average-position error (APE) [22] or mean-square-position error can be written as:

$$APE = \frac{\sum_{i=1}^{N} \sqrt{(\hat{\mathbf{a}}_i - \mathbf{a}_i)(\hat{\mathbf{a}}_i - \mathbf{a}_i)^\intercal}}{N} \tag{3}$$

where $\hat{\mathbf{a}}_i$ is the i-th localized module, $\mathbf{a}_i$ is its true position and N is the number of modules.

For a comparison of errors, based on the individual coordinates, five combinations of coordinates as inputs for the APE computation were used: xyz (3D), xy (2D), x, y and z coordinates. The notations of the APE for each coordinate combination are APE(xy), APE(x), APE(y) and APE(z), where the input argument presents the coordinates used for the APE computation. The APE without any input argument is used for the xyz combination.

For computing the APE, a rigid transformation has to be made to align the computing coordinates with the reference coordinates. The alignment is made with the least-square rigid-transformation method, described in [27]. The same method was used to align the localized CU from the measurements with a known position of the CU.

B. Localization methods

The aim of this paper was to analyze the impact of using the CU on the APE in 3D. To eliminate the effects of an incomplete Euclidean distance matrix (EDM) on the anchor-calibration accuracy, localization methods that use the complete EDM were used. A full EDM was constructed with measurements of all the inter-module distances. The only exceptions were the distances between the CM on the CU, which were computed from their known relative positions. One of the solutions for completing the EDM is described in [13], and another approach in [28], where smaller networks are joined if they have common modules in both sub-networks. We have used three localization algorithms: MDS [11], SDP [13] and TRI [14].

1) Multi-dimensional scaling: MDS is a mathematical method for reducing the dimensions of multi-dimensional data. For the localization, the data is usually reduced to two or three dimensions, depending on whether we are localizing in 2D or 3D space. MDS reduces the EDM to lower-dimensional data (coordinates) in such a way that the distances between the computed points represent the input EDM.

For the MDS localization algorithm, the steps described in [11] were used. Due to the anchor setup, there was no problem with computing the missing EDM entries as a first step of the localizing algorithm, since a full EDM could be obtained with measurements. For the second step, a MDS function implemented in Matlab was used. The third step was used for the APE computations, as the computed coordinates from the algorithm were aligned with the reference coordinates and for the actual anchor calibration method when the computed coordinates were aligned with the CU coordinates.

2) Semi-definite programming: For the second localization algorithm, the SDP algorithm from [13] was used. It uses semi-definite programming, i.e., a convex optimization procedure that minimizes the linear function. The optimized function is subjected to a constraint, such that the affine combination of symmetric matrices is positive semi-definite [29]. A general approach when using SDP for a localizing problem is using relaxation to solve:

$$\min_{\mathbf{Y} \succeq 0, \mathbf{Y} \in \mathbf{\Omega}} \|\mathbf{W} \circ (\kappa(\mathbf{Y}) - \mathbf{D})\|, \tag{4}$$

where $\mathbf{Y} \in \mathbf{\Omega}$ are linear restrictions, $\mathbf{Y}$ is the positive semi-definite matrix, $\mathbf{D}$ is the EDM, $\mathbf{W}$ is the weight matrix and $\circ$ is the Hadaman product [12].

3) Tri-lateration: The final method for anchor localization, TRI, is based on tri-lateration. Principles similar to the ones introduced in [14] were implemented. The TRI method uses $\binom{N}{4}$ different combinations of four initial anchors' combinations, where N is the number of anchors and CMs in the system. Each initial anchors' combination gives one anchor-calibration solution. The positions of the initial anchors are $\mathbf{a_1} = [0, 0, 0]^\intercal$, $\mathbf{a_2} = [d_{12}, 0, 0]^\intercal$, $\mathbf{a_3} = [a_{3x}, a_{3y}, 0]^\intercal$ and $\mathbf{a_4} = [a_{4x}, a_{4y}, a_{4z}]^\intercal$ with:

$$a_{3x} = \frac{d_{12}^2 + d_{13}^2 - d_{23}^2}{2d_{12}}, a_{3y} = \sqrt{d_{13}^2 - \frac{(d_{12}^2 + d_{13}^2 - d_{23}^2)^2}{4d_{12}^2}}, \tag{5}$$

$$a_{4x} = \frac{d_{12}^2 + d_{14}^2 - d_{24}^2}{2d_{12}}, a_{4z} = \sqrt{d_{14}^2 - (a_{4x}^2 + a_{4y}^2)},$$
$$a_{4y} = \frac{d_{12}(d_{13}^2 + d_{14}^2 - d_{34}^2) - a_{3x}(d_{12}^2 + d_{14}^2 - d_{24}^2)}{2d_{12}\ a_{3y}}. \tag{6}$$

This defines the coordinate system for a solution [30], where d_{12}, d_{13}, d_{14}, d_{23}, d_{24} and d_{34} are the distances between all four initial anchors.

After the initial anchors are localized, tri-lateration is used to localize all of the other anchors. Later, the number of initial anchors is reduced to shorten the computational time by discarding the co-planar combinations of the initial anchors. A threshold for co-planarity was determined so that the anchors on the same surface of the cuboid were eliminated. Also, additional initial anchor combinations were removed from any subsequent computation so as to achieve a reduction in the computation time of 60 %, without losing the accuracy of the anchors' coordinates. When all the suitable solutions of the anchor coordinates are computed, solutions with a stress parameter greater than a defined threshold are discarded. The algorithm output is a single set of anchor coordinates, which is an average value of the remaining solutions.

C. Simulation and experimental scenario layouts

To explore the anchor-calibration method with the CU, two scenario layouts were designed.

The first scenario (marked as GYM), presenting the LOS conditions with a symmetrical anchor placement, had 16 of a total of 18 modules placed on rectangular edges as anchors (Fig. 4). The experiments took place in a gym, where the modules were placed at two alternating heights along the borders of a rectangular field measuring 28 × 20 m. All 16 anchors were fixed on a wooden housing, so that they could be placed on top of telescopic stands.

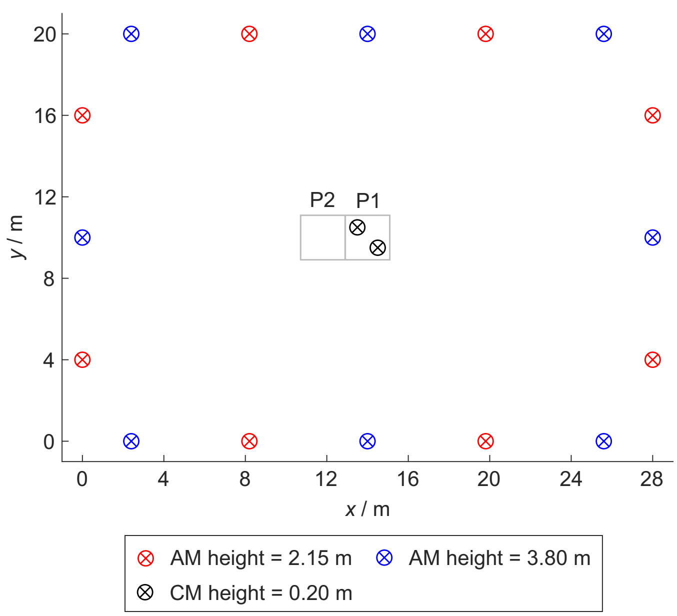

Fig. 4. Plane view of GYM scenario layout with 16 anchors and CU with 2 CM in optimal (P1) and non-optimal (P2) positions.

The second scenario (marked as LAB), had an asymmetrical placement of 12 anchors and NLOS conditions for several anchors pairs. The experiments were performed in the Laboratory of Robotics, which has a floor plan with dimensions of 10 × 12 m (Fig. 5), and is occupied by equipment and by people who are moving around. The anchors were placed at three different heights, so that the largest height difference was achieved. All 12 anchors were fixed to the wall with custom-designed wall mounts. The LAB scenario represents more complicated, realistic conditions, where the RTLS designer is limited by the range of suitable positions for the anchors.

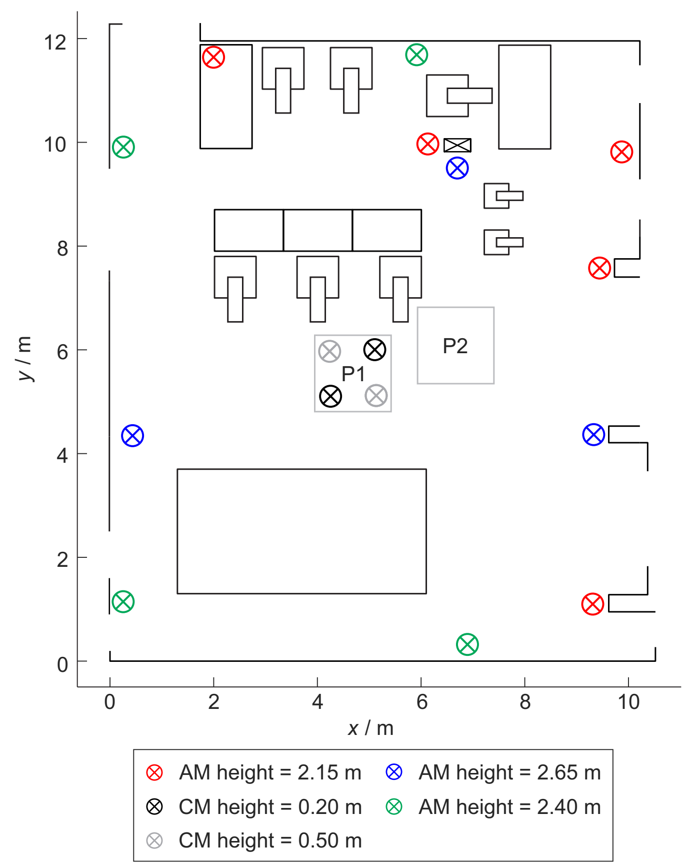

Fig. 5. Area with LAB scenario layout with 12 anchors and CU with 2 CM in optimal (P1) and non-optimal (P2) positions. The additional elements in the figure represent other objects in the laboratory.

The anchor-placement dimensions of both scenarios are presented in Table I. The maximum positional differences between the anchors are presented in the first three rows, and the last row presents the height difference between the highest anchors and the CU.

TABLE I
ANCHORS' MAXIMUM POSITIONAL DIFFERENCES FOR THE SCENARIOS GYM AND LAB.

	GYM	LAB
Δx / m	28	10
Δy / m	20	12
Δz / m	1.45	0.50
CUΔz / m	3.40	2.45

D. Anchor calibration

For the anchor calibration in the 3D working coordinate system at least four CMs on the CU are required. In the LAB scenario, an additional two calibration modules were added to opposite corners on the CU (light-gray markers in Fig. 5). When the relationship between the CU and the working coordinate system is known, the alignment of the localized anchor with respect to the CU is possible.

The CU is a square plate with an edge length of 1 m. The CMs are placed on its corners, as shown in Fig. 5. The positions of the CMs are measured, and with that, the relative positions with respect to the edges and corners of the CU plate are known. That way, CMs' coordinates P_{CM} are defined in the CU's coordinate system - P_{CM}^{CU}. When CU is positioned on WCS' reference points, the transformation between coordinate systems T is known. With $P_{CU}^{WCS} = TP_{CU}$ CMs coordinates can be transformed to WCS. The complete anchor-calibration procedure is presented in Fig. 6.

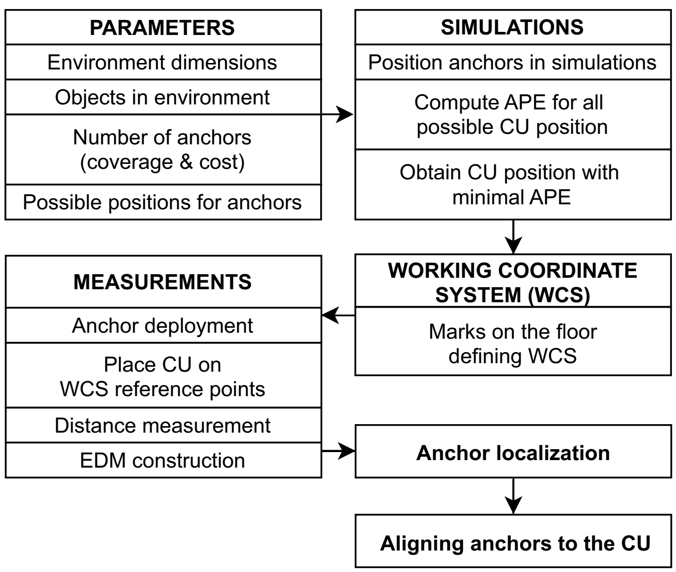

Fig. 6. Anchor calibration procedure flow chart.

E. Ground truth

Anchor-calibration method was evaluated experimentally with the measurement system. Ground-truth positions of the anchors were measured with a certified electronic tachymeter LeicaTPS 1201+, which represents the gold standard in reference-position measurements. The mounting plates for the anchors were designed in such a way that the reflective targets of the geodetic equipment could be fixed to them. After the geodetic measurements were made, the anchors were attached to the mounting plate with a known offset from the reflective target centre (the measured reference point). To obtain the true reference coordinates, the offsets between the coordinate of the reflective target's center and the anchor's antenna were applied to the reflective target's coordinates. In the second measurement series, wall mounts were designed for the anchors. The CU reference positions were measured in the same coordinate system as the anchor reference positions. The reference coordinates of the reflective targets were computed with an uncertainty of less than 1 mm.

V. Simulations

The following section describes the simulation configurations, parameters, and the corresponding results. The simulations were performed to evaluate the impact of the CU on the anchors' APE obtained using the three localization methods. The purpose of the simulations was to explore the different parameters of the CU before testing with the actual system. The conclusions drawn from the simulations were then used in the experiments.

A. Position of the calibration unit and the number of calibration modules

The tested parameters were the number of CMs used and their positions. The notation for the different numbers of CMs is AX, where X is the number of CMs on the CU. All the configurations are presented in Fig. 7, where the crossed black circles represent one CM on a CU. Each gray square's side has a length of 1 m. Simulations were made for each CU configuration. In the simulations, the CU position (red cross in Fig. 7) changed in the x, y and z coordinates of the GYM or LAB area (Fig. 4 and 5), as described in Table II. To evaluate the impact of the CU on the anchor localization, a configuration without a CU, indicated as A0, was used. In the simulations, the noise was modelled with a Gaussian zero-mean random variable, which had a standard deviation of 0.15 m [24]. The same set of random seed numbers was used for all three localization methods in 100 simulation runs. For the APE calculation, only the positions of the anchors were used.

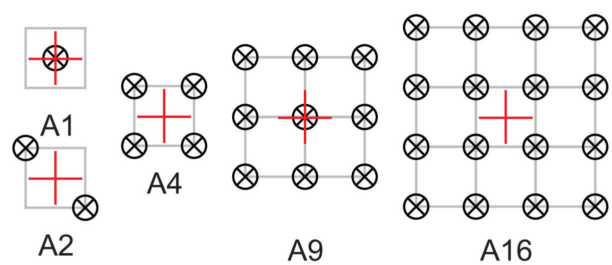

Fig. 7. Configuration of the calibration modules used in the simulations.

TABLE II
CU position ranges for the scenarios GYM and LAB in simulations.

	GYM	LAB	
x / m	0–28.0	0–8.0	step 1.0 m
y / m	0–20.0	0–10.5	step 1.0 m
z / m	0–2.0	0–2.0	step 0.2 m

The results from 100 simulation runs were averaged so that a single APE value was obtained for each CU position. From all of the CU positions, the one with the smallest APE was chosen as the final result presented in Table III.

This article has been accepted for publication in a future issue of this journal, but has not been fully edited. Content may change prior to final publication. Citation information: DOI 10.1109/TIM.2020.3005258, IEEE Transactions on Instrumentation and Measurement

For the A1 configuration the APE was 28 % and 26 % lower compared to A0 configuration, when using the MDS and the TRI methods in the GYM scenario. In the LAB scenario, the APE was 76 % and 47 % lower. When the maximum number of CMs was added (A16 configuration), the APE was lowered by 62 % and 34 % compared to the A0 configuration, for the MDS and TRI methods in the GYM scenario. In the LAB scenario, the APE was lowered by 87 % and 65 %, when using the MDS and the TRI method. APE improvements for the selected A2 configuration are presented in the bottom row of Table III. Compared to the other two methods, the SDP method had significantly higher APE values in the A0 configurations. This method proved to be noise sensitive, especially in the A0 configuration. When using the CU with the SDP method, simulations had better results and the trend of the decreasing APE with respect to the additional CMs can be seen in Table III, from the A1 configuration onward.

TABLE III
APE OBTAINED BY SIMULATIONS FOR THE A0, A1, A2, A4, A9 AND A16 SIMULATION CONFIGURATIONS FOR ALL 3 LOCALIZATION METHODS FOR THE SCENARIOS GYM AND LAB.

	GYM			LAB		
	MDS	SDP	TRI	MDS	SDP	TRI
A0 / m	0.039	0.237	0.047	0.084	0.171	0.095
A1 / m	0.028	0.018	0.035	0.020	0.017	0.050
A2 / m	0.025	0.017	0.036	0.017	0.015	0.048
A4 / m	0.020	0.016	0.031	0.014	0.011	0.037
A9 / m	0.017	0.013	0.030	0.012	0.010	0.035
A16 / m	0.015	0.011	0.031	0.011	0.009	0.033
ΔA2 / m	0.014	0.220	0.011	0.068	0.156	0.047

The biggest APE improvement per number of used CMs was seen when using the A1 configuration. The improvement with the MDS and TRI methods was 0.011 m/CM and 0.012 m/CM for the GYM scenario and 0.064 m/CM and 0.045 m/CM for the LAB scenario. For the A2 configuration, the APE improvement per CM was 50 % smaller, compared to the A1 configuration. The only exception was in the GYM scenario and with the MDS method, where the APE was improved by 64 %. For the A4 configuration the improvements were less than 30 %, for the A9 configuration less then 15 % and for the A16 configuration less then 10 % of those seen in the A1 configuration.

The surf plot in Fig. 8 illustrates how changes in the CU position affect the APE values, for the A2 configuration and the TRI method. From all the positions verified in the simulations, the smallest APE value along the z coordinate was selected for this plot. All three localization methods had a similar spherical shape of error, but different absolute values. The APE was the smallest when the CU was in the central position for the GYM scenario, and outside of it for the LAB scenario. In the LAB scenario, localization methods had smaller deviations of the CU position for up to 0.5 m. The smallest APE values from simulations of the A2 configuration are presented in Table III. Optimal positions for both scenarios are presented in Fig. 4 and 5.

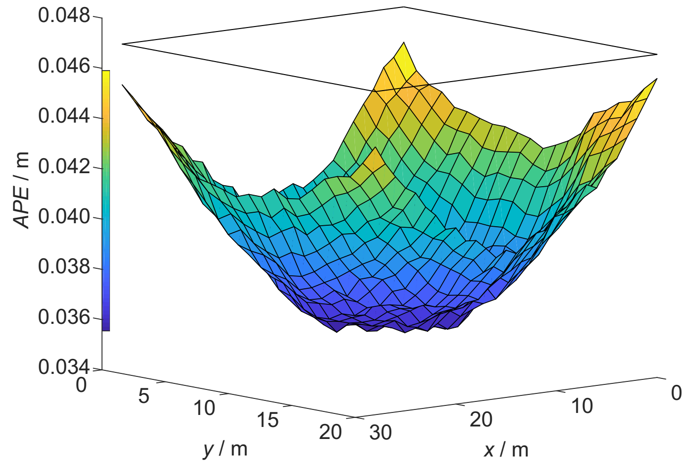

Fig. 8. The A2 simulation results (surf plot) and a result of the A0 simulation (black square), for the TRI localization method. Values on the surf plot represent the smallest average APE along the z-axis. The presented values in the figure are average values computed from 100 simulation runs for each x, y, and z coordinate.

B. Height difference between the anchors and the calibration unit

Simulations were used to evaluate how different height differences along the z coordinate between the anchors and the CU impact on the anchors' APE. Height-difference simulations used the x and y coordinates from the positions with the smallest APE, acquired from previous simulations. The height difference was increased throughout the simulation, up to 28 m in the GYM scenario and 12 m in the LAB scenario. With these values, the height differences between the anchors and the CMs were the same as the longest edge of the anchor's floor layout (Table I). These conditions provide better spatial information for the anchor calibration, as additional calibration modules improve the co-planarity of the anchor configuration.

The APE results of the simulations for six different heights are shown in Table IV. In the GYM scenario, the APE improvement was the greatest in the range of height differences up to 15.0 m. This is approximately half the length of the longest edge of the anchor's floor layout. For this height difference, the APE declined by 60 % with the MDS, 53 % with the SDP, and 58 % with the TRI method, compared to the APE in the A2 configuration from Table III.

TABLE IV
APE OBTAINED BY A2 SIMULATIONS WHERE THE HEIGHT DIFFERENCE BETWEEN THE CU AND THE HIGHEST ANCHOR WAS INCREASED FOR THE OPTIMAL X AND Y POSITIONS.

	distances / m	3.6	5.0	10.0	15.0	20.0	28.0
GYM	MDS / m	0.025	0.020	0.012	0.010	0.009	0.009
	SDP / m	0.017	0.014	0.010	0.008	0.008	0.007
	TRI / m	0.036	0.029	0.018	0.015	0.014	0.014
	distances / m	2.7	3.1	2.7	5.1	6.5	12.0
LAB	MDS / m	0.015	0.014	0.012	0.011	0.010	0.009
	SDP / m	0.014	0.012	0.011	0.009	0.009	0.008
	TRI / m	0.048	0.029	0.016	0.013	0.012	0.015

This article has been accepted for publication in a future issue of this journal, but has not been fully edited. Content may change prior to final publication. Citation information: DOI 10.1109/TIM.2020.3005258, IEEE Transactions on Instrumentation and Measurement

In the LAB scenario, the APE improvement was the largest in the range of height differences up to 5.1 m, which is again approximately half the length of the longest edge of the anchor's floor layout. For the height difference of 5.1 m, the APE declined by 27 % with the MDS, 36 % with the SDP, and 67 % with the TRI method, compared to the APE in the A2 configuration from Table III.

VI. EXPERIMENTAL RESULTS

The following section presents the experimental results. First, the improvement of the anchors' APE, using an additional CU with two CMs, for both scenarios and two CU positions, is presented. Finally, the results of the anchor calibration, by means of alignment with the CU, are presented with the use of four CMs on the CU for two positions in the LAB scenario.

A. Improving the APE with a calibration unit

A test on the real anchor network system was performed to test anchor's network system, validate simulation results, confirm the use of simulations for determining the optimal CU position, and validate the anchor calibration method. Due to the number of anchors used in the GYM scenario, the test used A2 configuration and positions, obtained using prior simulations.

In the GYM scenario, the APE improved by 0.01 m with the MDS, 0.03 m with the SDP, and 0.01 m with the TRI method (Table V). In the LAB scenario, the APE improved by 0.30 m with the MDS, 0.23 m with the SDP, and 0.10 m with the TRI method. In both scenarios the MDS method had the lowest APE for the A0 and A2 configurations. The SDP and TRI methods had similar APE values for the A2 configuration in both scenarios, with a difference of 0.01 m. The MDS method gave results with the APE that were two-times smaller in the GYM and 1.5-times smaller in the LAB scenario, compared to the SDP and TRI methods.

TABLE V
EXPERIMENTAL APE FOR FIRST POSITION OF CU FOR ANCHOR LOCALIZATION WHEN A0 AND A2 IS USED, FOR BOTH SCENARIOS.

	GYM			LAB		
	MDS	SDP	TRI	MDS	SDP	TRI
A0 / m	0.08	0.17	0.14	0.44	0.45	0.33
A2 / m	0.07	0.14	0.13	0.14	0.22	0.23
Δ / m	0.01	0.03	0.01	0.30	0.23	0.10

The average APEs were calculated from 40 measurement sets for the xyz, xy, x, y, and z coordinates for all three localization methods, for the GYM scenario (Fig. 9) and for the LAB scenario (Fig. 10). The APE was smaller with the CU deployed, regardless of the localization method used (all the blue marks are under the red marks).

In the GYM scenario, the standard deviations (STDs) of the APEs were below 0.01 m for APE and APE(z), and below 0.002 m for APE(xy), APE(x), and APE(y) for the A0 and A2 configurations and all three localization methods.

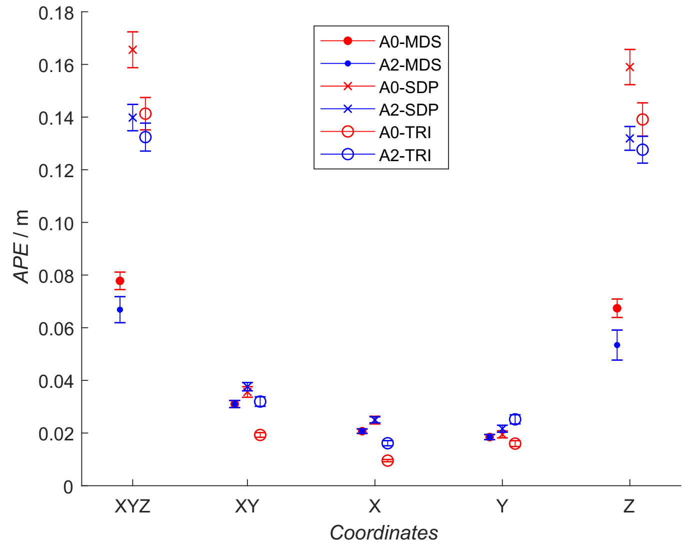

Fig. 9. Mean APE values computed from 40 measurement sets, for all the localization methods and $A0$ and $A2$ configurations, with the standard deviation for the GYM scenario. Results are displayed as a function of the coordinates xyz, yx, x, y, and z, used for the APE calculation.

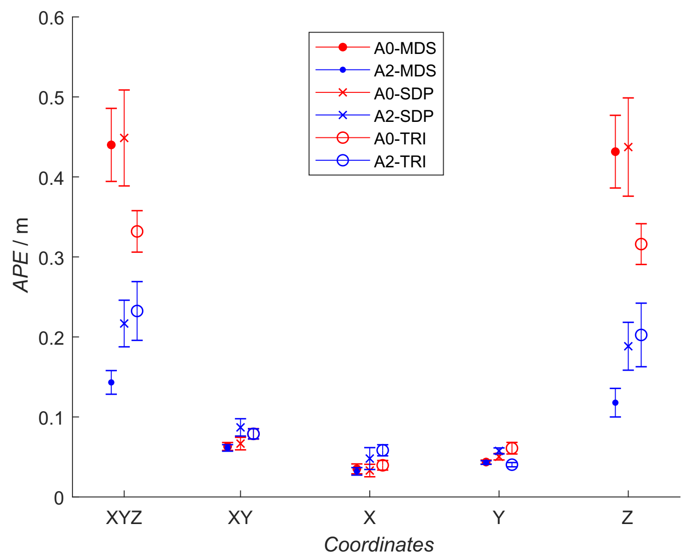

Fig. 10. Mean APE values computed from 40 measurement sets, for all the localization methods and $A0$ and $A2$ configurations, with the standard deviation for the LAB scenario. Results are displayed as a function of the coordinates xyz, yx, x, y, and z, used for the APE calculation.

In the LAB scenario, the STDs of the APEs were different for the A0 and A2 configurations and all three localization methods. The STDs of the APE and APE(z) for the A0 configuration were below 0.05 m for the MDS, 0.06 m for the SDP, and 0.03 m for the TRI method (Fig. 10 - red marks). The STDs of the APE and APE(z) for the A2 configuration were 0.02 m for the MDS, 0.03 m for the SDP, and 0.04 for the TRI method (Fig. 10 - blue marks). The STDs of APE(xy), APE(x), and APE(y) were below 0.01 m for all the localization methods and both configurations.

The difference between APE and APE(z) in the GYM scenario was smaller than 0.01 m for the MDS and the SDP methods and smaller than 0.005 m for the TRI method for the A0 and A2 configurations. The difference between the APE and APE(z) in the LAB scenario was 0.01 m with the MDS and the SDP methods, and smaller than 0.005 m with the TRI method for the A0 configuration. However, for the A2 configuration, the differences between APE and APE(z) were 0.03 m with all three methods. For a further analysis of APE(xy), APE(x), APE(y), and APE(z) from the data in Fig. 9 and 10 were normalized with the APE. In this case APE(z) represents over 90 % of the APE and APE(xy),APE(x), and APE(y) represent, on average, 21 % of the APE.

B. Non-optimal position of the calibration unit

To confirm the APE improvement utilizing the CU, additional measurements with the CU in different positions were made. The CU was moved from the non-optimal position P2 to the optimal position P1 for both scenarios presented in Fig. 4 and 5.

In the GYM scenario, the APE decreased by 0.01 m with the MDS, 0.02 m with the SDP and with the TRI method when implementing the A2 instead of the A0 configuration (Table VI). In the LAB scenario, the APE decreased by 0.25 m with the MDS, 0.20 m with the SDP, and 0.07 m with the TRI method.

TABLE VI
EXPERIMENTAL APE FOR SECOND POSITION OF CU FOR ANCHOR LOCALIZATION WHEN A0 AND A2 IS USED, FOR BOTH SCENARIOS.

	GYM			LAB		
	MDS	SDP	TRI	MDS	SDP	TRI
A0 / m	0.08	0.16	0.14	0.41	0.41	0.32
A2 / m	0.07	0.14	0.12	0.16	0.21	0.25
Δ / m	0.01	0.02	0.02	0.25	0.20	0.07

A comparison of the values from Table V and Table VI for the LAB scenario, shows smaller APE improvements when the CU was used in the non-optimal position, compared to the optimal one. On average, the improvement in the non-optimal position was more than 0.03 m less than in the optimal position, for all the localization methods in the LAB scenario. In the GYM scenario, the APE values for the A2 configuration are the same. The only exception was with the TRI method, which had a 0.01 m larger APE in the non-optimal position. The APE values were almost two-times-higher in NLOS conditions (LAB) than in LOS conditions (GYM).

The mean-bias error of the measured distances and the mean standard deviation, calculated from 40 measurement sets, are presented in Table VII. The NLOS conditions in the LAB scenario gave an almost two-times-higher mean error and a more than two-times-higher standard deviation, in comparison to the LOS conditions in the GYM scenario.

C. Anchor calibration in the working coordinate system

To assess the presented anchor-calibration method with the CU, a test of the anchor localization in the working coordinate system was conducted. It used four CMs on the CU in the

TABLE VII
MEAN ERROR AND STD FOR MEASURED DISTANCES FOR THE GYM AND LAB SCENARIO IN THE OPTIMAL POSITION (P1).

	GYM	LAB
Bias / m	0.06	0.10
Std / m	0.05	0.13

TABLE VIII
ANCHOR-CALIBRATION RESULTS, ALIGNMENT WITH KNOWN CALIBRATION-MODULE POSITIONS.

		MDS	SDP	TRI
P1	A4 / m	0.32	0.36	1.06
P2	A4 / m	0.44	0.40	1.40

LAB scenario, with the CU in two positions, i.e., optimal and non-optimal, as presented as P1 and P2 in Fig. 4 and 5. In the optimal position P1, the APE values were smaller compared to the non-optimal position P2. They decreased by 0.12 m, 0.04 m, and 0.34 m, with the MDS, SDP, and TRI methods (Table VIII).

VII. DISCUSSION

Previous work introduced the use of a calibration unit (CU) as a feature to interconnect multiple anchors. This is beneficial if the anchors do not have a ranging capability due to obstacles or out-of-range distances between the anchors. This paper presents an anchor-calibration method that uses additional calibration modules (CMs) to improve the anchor localization and also localize the anchors in a working coordinate system. First, it was shown through simulations that the anchor-calibration accuracy can be improved by adding a feature, such as a CU. Second, the simulation results were validated with an experiment on a real system in 3D. Finally, an anchor calibration in a working coordinate system in 3D was performed and evaluated.

The simulation results showed a decrease of the APE for both scenarios and all the localization methods, when additional CMs were used (Table. III). When comparing the APE improvement as an absolute value per added CM, the A1 configuration had the best results. Compared to the best A16 configuration, the values were over 7 times lower with the MDS method, and over 12 times lower when using the SDP and TRI methods. Even though the APE decreased further with more CMs used, the growing number of CMs raises the overall price and complexity of the system. It is worth noting that the APE improvement did not change linearly, but decreased exponentially when the number of newly added CMs increased. Therefore, the optimal number of CMs used should be determined by the permissible APE value and the available resources. Simple square shape simulation configurations were chosen so that they could be easily replicated for the experiment.

Another parameter that could possibly improve the accuracy of the anchor coordinates is the height difference between the anchor and the CM. The height of the anchor placement was limited in the real-life experiments; however, it was possible to

This article has been accepted for publication in a future issue of this journal, but has not been fully edited. Content may change prior to final publication. Citation information: DOI 10.1109/TIM.2020.3005258, IEEE Transactions on Instrumentation and Measurement

avoid and overcome those limitations through simulations. The height difference was increased to the height that corresponded to the length of the edges of the anchor's floor layout. These outer boundaries on the floor, described by the positions of the anchors, are shown in Fig. 4 and 5 and in Table I. The simulation results showed that increasing the height difference between the anchors and the CM, reduced the values of the APE (Table IV). This reduction was seen up to the point where the height difference was equal to the length of one-half of the anchor's floor-layout edge.

The experiments in GYM and LAB confirmed that the APE could be reduced by including the CU in the measurement. In the GYM scenario, the APE values decreased by at least 0.01 m and in the LAB by 0.07 m, with the TRI method, to 0.30 m, with the MDS method (Table V and VI). Simulation results predicted a greater reduction of the APE for the LAB scenario, which the experimental results confirmed (Table III). Of course, the simulation and experimental APE values differ, the main reasons could be that the simulations used a noise model without any bias. Those differences could be reduced in subsequent research by implementing a model that includes a nonlinear bias error of the distance measurements, the NLOS conditions, and the dependency of the measured distance on the anchors' orientations. The APE reductions with the SDP method were not directly compared, due to the problems (see next paragraph) with the A0 configuration simulations. Those problems resulted in poor localization and, consequently, the simulation data gave much larger APE values than the experimental data.

When comparing the simulated and experimental results for the A2 configuration, obtained with the MSD and SDP methods, differences in the performance arose. In simulations, the SDP had smaller APE values than the MDS method. However, the experiments yielded contrasting results. As mentioned, the SDP method proved to be noise sensitive. In additional simulations, the distances included the bias error. If there was no additional bias error present, the SDP method gave better results. However, its performance reduced faster, compared to the MDS method, when the mean-bias error increased. For the values of the mean-bias error present in the experiments, the MDS method outperformed the SDP method.

A comparison of the errors for all the coordinate combinations showed that the largest contribution to the APE came from the error along the z-axis (Fig. 9 and 10). When the CU was utilized, the APE decreased, with the largest change being on the z-axis. Small STD values of the mean APE value in the GYM scenario indicates that our anchor system and the presented anchor-calibration procedure are stable. In the LAB scenario, with the NLOS and time-varying conditions, larger STD values were present. NLOS conditions in LAB scenario, along with setup configuration, resulted in larger APE values (Table V and VI). In the GYM scenario with LOS conditions, and therefore smaller bias error and STD in distance measurements (Table VII), a smaller number of measurement sets can be used for anchor calibration. The number of measurement sets should be increased for more severe NLOS conditions, as in the LAB scenario, within time constraints. With a bigger number of measurement sets, rather than measured distances in each set, different conditions are recorded for all anchor pairs.

The results obtained for the LAB scenario (Table V and VI) confirmed that the optimal position can be attained through simulations, where the APE improvement is smaller in the non-optimal position. Therefore, the simulations are a suitable tool to evaluate the optimal position in both simple and more complex environments. Results from GYM scenario did not provide the APE difference between different position, due to the relatively small position change of CU in bigger anchor layout. Due to the complexity associated with anchor configuration, it is difficult to generalize the CU setup options. Experimental results have shown that a larger height difference between the anchors and the CU, and between the anchors themselves, gives better localization results. However, both parameters are usually limited by the realistic environment where the RTLS will operate. The APE results of both scenarios and both positions showed that the MDS localization method is the most suitable for our anchor-calibration method.

The results of the anchor calibration from previous research and from this paper are compared in Table IX. All the presented error values are associated with aligning the localized anchors with their reference positions in 2D. Through this, the performance of anchor-calibration methods can be evaluated, even though the anchors are not placed in a coordinate system where the RTLS could operate. The results are comparable with the first part of this paper, where the effects of the CU on the anchor calibration were studied. When comparing the results within the Table IX, parameters such as the anchor configuration and the number of anchors, have to be taken into consideration. The APE values show the good performance of the presented calibration method, in simple LOS as well as in NLOS conditions, and complex, more realistic environments.

TABLE IX
AVERAGE 2D POSITIONAL ERROR FOR ANCHOR CALIBRATION IN PREVIOUS RESEARCH AND THIS PAPER.

	no. anchors (no. CM)	2D / m	3D / m
Nakamura *et al.* [21]	8 (0)	0.95	/
Müller *et al.* [23]	4 (1)	1.20	/
Van de V. *et al.* [24]	4 (1)	0.08	/
Scenario GYM	16 (2)	0.03	0.07
Scenario LAB	12 (2)	0.06	0.14

The presented anchor calibration method is a useful tool for RTLS initialization without external measurement equipment. In cases with hybrid systems [5], it would be beneficial as calibration of the UWB system also calibrates primary systems. Where RTLS uses smaller anchor systems method enables fast reconfigurability [6]. In industrial environments, the calibration method provides possibilities of merging coordinate systems of different RTLS based on different technologies and covering different areas [7], [8].

Finally, the proposed anchor-calibration method was tested in a real experiment, where a setup of 12 anchors and 4 CMs on the CU, in the desired working coordinate system, was placed. In this way the alignment of the localized anchor to the work coordinate system was possible. With the MDS method, an anchor calibration with a 3D error of 0.32 m was achieved.

VIII. Conclusion

This paper presents a novel approach to a self-localizing anchor-system calibration that uses a calibration unit for improved localization accuracy. This study confirmed that the use of the calibration unit decreases the average positional error of the anchors in 3D localization systems. Additionally, the simulations were confirmed to be a valid tool for determining the best position of the calibration unit. Finally, the first demonstration of an anchor calibration with a calibration unit and anchors localized in the working coordinate system in 3D was presented. It had an error of 0.32 m.

The performance of the three different localization methods was tested and the results showed that the multi-dimensional scaling method had the best localization accuracy. Using a calibration unit enables all the applications to improve the anchor-localization accuracy. The potential downside of using a calibration unit for the anchor calibration is the need to use additional modules, affecting the complexity and the price of the localization system.

In future work an analysis of the effects of adding a calibration unit to anchor configurations, where a complete Euclidean distance matrix (EDM) cannot be assembled from mere measurements, would be beneficial. For the EDM completion, additional steps in the localization algorithms should be taken. This would enable the localization of all the anchors in the RTLS, and consequently, the anchor calibration could be used universally for almost all RTLS applications and their specific environmental requirements.

Acknowledgment

The authors acknowledge the financial support from Slovenian Research Agency (research core funding No. P2-0228) and young researcher founding. This research was funded by the European Commission under the CYBERLEGs Plus Plus project (Grant #731931), within the H2020 framework (H2020-ICT-25-2016-2017). The authors would like to thank assist. G. Štebe M.S. from the Faculty of Civil and Geodetic Engineering for the reference-point measurements and B. Jakopin for his valuable comments during the preparation of this paper.

References

[1] K. Guo, Z. Qiu, C. Miao, A. H. Zaini, C.-L. Chen, W. Meng, and L. Xie, "Ultra-wideband-based localization for quadcopter navigation," *Unmanned Syst.*, vol. 4, no. 1, pp. 23–34, Feb. 2016.

[2] X. Tang and S. Mandal, "Indoor occupancy awareness and localization using passive electric field sensing," *IEEE Trans. Instrum. Meas.*, vol. 68, no. 11, pp. 4535–4549, Nov 2019.

[3] A. R. JimÃľnez Ruiz and F. Seco Granja, "Comparing ubisense, bespoon, and decawave uwb location systems: Indoor performance analysis," *IEEE Trans. Instrum. Meas.*, vol. 66, no. 8, pp. 2106–2117, Apr. 2017.

[4] S. He and X. Dong, "High-accuracy localization platform using asynchronous time difference of arrival technology," *IEEE Trans. Instrum. Meas.*, vol. 66, no. 7, pp. 1728–1742, Mar. 2017.

[5] M. Kolakowski, "A hybrid ble/uwb localization technique with automatic radio map creation," in *2019 13th Eur. Conf. Antennas and Propagation (EuCAP)*, Krakow, Poland, Jun. 2019, pp. 1–4.

[6] J. Wang, Y. Tang, J. Muñoz-Ferreras, R. Gómez-García, and C. Li, "An improved indoor localization solution using a hybrid uwb-doppler system with kalman filter," in *2018 IEEE Radio and Wireless Symposium (RWS)*, Anaheim, CA, USA, Mar. 2018, pp. 181–183.

[7] A. Martinelli, S. Jayousi, S. Caputo, and L. Mucchi, "Uwb positioning for industrial applications: the galvanic plating case study," in *2019 Int. Conf. Indoor Positioning and Indoor Navigation (IPIN)*, Pisa, Italy, Nov. 2019, pp. 1–7.

[8] W. Wang, Z. Zeng, W. Ding, H. Yu, and H. Rose, "Concept and validation of a large-scale human-machine safety system based on real-time uwb indoor localization*," in *2019 IEEE/RSJ Int. Conf. Intelligent Robots and Systems (IROS)*, Macau, China, Jan. 2019, pp. 201–207.

[9] C. Zhou, T. Xu, and H. Dong, "Distributed locating algorithm MDS-MAP (LF) based on low-frequency signal," *Comput. Sci. Inf. Syst.*, vol. 12, no. 4, pp. 1289–1305, Nov. 2015.

[10] W. Cui, C. Wu, W. Meng, B. Li, Y. Zhang, and L. Xie, "Dynamic multidimensional scaling algorithm for 3-d mobile localization," *IEEE Trans. Instrum. Meas.*, vol. 65, no. 12, pp. 2853–2865, Dec 2016.

[11] Y. Shang, W. Rumi, Y. Zhang, and M. Fromherz, "Localization from connectivity in sensor networks," *IEEE Trans. Parallel Distrib. Syst.*, vol. 15, no. 11, pp. 961–974, Nov. 2004.

[12] N. Krislock and H. Wolkowicz, "Explicit sensor network localization using semidefinite representations and facial reductions," *SIAM J. Optim.*, vol. 20, no. 5, pp. 2679–2708, Jan. 2010.

[13] D. Drusvyatskiy, N. Krislock, Y.-L. Voronin, and H. Wolkowicz, "Noisy Euclidean distance realization: robust facial reduction and the Pareto frontier," *SIAM J. Optim.*, vol. 27, no. 4, pp. 2301–2331, Oct. 2017.

[14] D. K. Goldenberg, P. Bihler, M. Cao, J. Fang, B. Anderson, A. S. Morse, and Y. R. Yang, "Localization in sparse networks using sweeps," in *Proc. 12th Annu. Int. Conf. Mobile Computing and Networking*, Los Angeles, CA, USA, Sep. 2006, pp. 110–121.

[15] N. B. Priyantha, H. Balakrishnan, E. Demaine, and S. Teller, "Anchor-free distributed localization in sensor networks," in *Proc. 1st Int. Conf. Embedded Networked Sensor Systems*, Los Angeles, CA, USA, Nov. 2003, pp. 340–341.

[16] A. Savvides, C.-C. Han, and M. B. Strivastava, "Dynamic fine-grained localization in ad-hoc networks of sensors," in *Proc. 7th Annu. Int. Conf. Mobile Computing and Networking*, Rome, Italy, Jul. 2001, pp. 166–179.

[17] Y. Kuang, S. Burgess, A. Torstensson, and K. Åström, "A complete characterization and solution to the microphone position self-calibration problem," in *2013 IEEE Int. Conf. Acoustics, Speech and Signal Processing (ICASSP)*, Vancouver, BC, Canada, May 2013, pp. 3875–3879.

[18] K. Batstone, M. Oskarsson, and K. Åström, "Towards real-time time-of-arrival self-calibration using ultra-wideband anchors," in *2017 Int. Conf. Indoor Positioning and Indoor Navigation (IPIN)*, Sapporo, Japan, Sep. 2017, pp. 1–8.

[19] Y. Zhou, C. L. Law, and F. Chin, "Construction of local anchor map for indoor position measurement system," *IEEE Trans. Instrum. Meas.*, vol. 59, no. 7, pp. 1986–1988, Jul. 2010.

[20] P. Duff and H. L. Muller, "Autocalibration algorithm for ultrasonic location systems," in *7th Int. Symp. Wearable Computers*, vol. 3, White Plains, NY, USA, Oct. 2003, p. 62.

[21] K. Nakamura and K. Sakamura, "Sub-meter accuracy localization system using self-localized portable uwb anchor nodes," in *1st IEEE Global Conf. Consumer Electronics 2012*, Tokyo, Japan, Oct. 2012, pp. 695–698.

[22] D. Moore, J. Leonard, D. Rus, and S. Teller, "Robust distributed network localization with noisy range measurements," in *Proc. 2nd Int. Conf. Embedded Networked Sensor Systems*, Baltimore, MD, USA, Nov. 2004, pp. 50–61.

[23] M. Müller, J. Lategahn, L. Telle, and C. Röhrig, "Automatic anchor calibration in IEEE 802.15. 4a networks," in *2011 8th Workshop Positioning Navigation and Communication*, Dresden, Germany, Apr. 2011, pp. 67–71.

[24] S. Van de Velde, P. Van Torre, and H. Steendam, "Fast and robust anchor calibration in range-based wireless localization," in *2013 7th Int. Conf. Signal Processing and Communication Systems (ICSPCS)*, Gold Coast, Australia, Dec. 2013, pp. 1–6.

[25] D. Neirynck, E. Luk, and M. McLaughlin, "An alternative double-sided two-way ranging method," in *2016 13th Workshop Positioning, Navigation and Communications (WPNC)*, Bremen, Germany, Oct. 2016, pp. 1–4.

[26] A. Cazzorla, G. De Angelis, A. Moschitta, M. Dionigi, F. Alimenti, and P. Carbone, "A 5.6-GHz UWB position measurement system," *IEEE Trans. Instrum. Meas.*, vol. 62, no. 3, pp. 675–683, Mar. 2013.

This article has been accepted for publication in a future issue of this journal, but has not been fully edited. Content may change prior to final publication. Citation information: DOI 10.1109/TIM.2020.3005258, IEEE Transactions on Instrumentation and Measurement

[27] K. S. Arun, T. S. Huang, and S. D. Blostein, "Least-squares fitting of two 3-D point sets," *IEEE Trans. Pattern Anal. Mach. Intell.*, vol. PAMI-9, no. 5, pp. 698–700, Sep. 1987.

[28] Y. Shang and W. Ruml, "Improved mds-based localization," in *IEEE INFOCOM 2004*, vol. 4, Hong Kong, China, Mar. 2004, pp. 2640–2651.

[29] L. Vandenberghe and S. Boyd, "Semidefinite programming," *SIAM Rev.*, vol. 38, no. 1, pp. 49–95, Mar. 1996.

[30] F. Santos, "Localization in wireless sensor networks," *ACM J*, vol. 5, pp. 1–19, Nov. 2008.